Coupling of narrow and wide band-gap semiconductors on uniform films active in bacterial disinfection under low intensity visible light: Implications of the interfacial charge transfer (IFCT)

S. Rtimi [a,b,*], R. Sanjines [c], C. Pulgarin [a,**], A. Houas [b], J.-C. Lavanchy [d], J. Kiwi [e]

[a] Ecole Polytechnique Fédérale de Lausanne, EPFL-SB-ISIC-GPAO, Station 6, CH-1015 Lausanne, Switzerland
[b] UR Catalyse/Matériaux pour l'Environnement et les Procédés (URCMEP), Faculté des Sciences de Gabès, Université de Gabès, 6072 Gabès, Tunisia
[c] Ecole Polytechnique Fédérale de Lausanne, EPFL-SB-IPMC-LNNME, Bat PH, Station 3, CH1015 Lausanne, Switzerland
[d] Université de Lausanne, IMG, Centre d'Analyse Minérale, Bat Anthropole, CH-1015 Lausanne, Switzerland
[e] Ecole Polytechnique Fédérale de Lausanne, EPFL-SB-ISIC-LPI, Bat Chimie, Station 6, CH1015 Lausanne, Switzerland

HIGHLIGHTS

- Design, preparation, testing and characterization of uniform sputtered films.
- Interfacial charge transfer from the Ag$_2$O (cb) to the lower laying Ta$_2$O$_5$ (cb).
- The optical absorption of TaON and TaON/Ag was proportional to *E. coli* inactivation.
- Self-cleaning of the TaON/Ag polyester enables repetitive *E. coli* inactivation.

ARTICLE INFO

ABSTRACT

This study reports the design, preparation, testing and surface characterization of uniform films deposited by sputtering Ag and Ta on non-heat resistant polyester to evaluate the *Escherichia coli* inactivation by TaON, TaN/Ag, Ag and TaON/Ag polyester. Co-sputtering for 120 s Ta and Ag in the presence of N$_2$ and O$_2$ led to the faster *E. coli* inactivation by a TaON/Ag sample within ∼40 min under visible light irradiation. The deconvolution of TaON/Ag peaks obtained by X-ray photoelectron spectroscopy (XPS) allowed the assignment of the Ta$_2$O$_5$ and Ag-species. The shifts observed for the XPS peaks have been assigned to AgO to Ag$_2$O and Ag^0, and are a function of the applied sputtering times. The mechanism of interfacial charge transfer (IFCT) from the Ag$_2$O conduction band (cb) to the lower laying Ta$_2$O$_5$ (cb) is discussed suggesting a reaction mechanism. The optical absorption of the TaON and TaON/Ag samples found by diffuse reflectance spectroscopy (DRS) correlated well with the kinetics of *E. coli* inactivation. The TaON/Ag sample microstructure was characterized by contact angle (CA) and by atomic force microscopy (AFM). Self-cleaning of the TaON/Ag polyester after each disinfection cycle enabled repetitive *E. coli* inactivation.

© 2013 Elsevier B.V. All rights reserved.

1. Introduction

Antimicrobial surfaces reduce or eliminate hospital-acquired infections (HAI) due to antibiotic resistant bacteria that survive nowadays on hospital surfaces for long times [1]. More effective antibacterial films are needed at present due to the increasing resistance of pathogenic bacteria to synthetic antibiotics when administered for long times [2]. Recently, Mills et al. [3], Parkin et al. [4–7], Foster et al. [8], Dunlop et al. [9] and Yates et al. [10] have reported antibacterial films of Ag and Cu films on glass and thin polymer films by chemical vapor deposition (CVD) and in some cases sputtering techniques.

Most of the semiconductors have too large band-gaps to absorb visible light. This is because their band-gap consists mainly of O2p orbitals with energies of about *ca.* 3 eV. Recently studies have shown that the optical absorption of TiO$_2$ can be shifted toward the visible range by introducing mid-gap levels above the top of the O2p valence band by addition of nitrogen [11]. This study presents details of the coupling of a small bang-gap semiconductor Ag$_2$O (bg ∼ 1.5 eV) absorbing visible light being coupled with a large band semiconductor Ta$_2$O$_5$ (bg ∼ 4.0 eV).

The sputtering of oxides/nitrides allows the preparation of adhesive films, which are mechanically stable and superior to films

* Corresponding author at: Ecole Polytechnique Fédérale de Lausanne, EPFL-SB-ISIC-GPAO, Station 6, CH-1015 Lausanne, Switzerland. Tel.: +41 21 693 6150.
** Corresponding author. Tel.: 041 21 693 4720.
E-mail addresses: sami.rtimi@epfl.ch (S. Rtimi), cesar.pulgarin@epfl.ch (C. Pulgarin).

prepared by deposition of colloid/powders, which can be readily wiped off using a cloth or thumb [12]. Our laboratory has recently reported oxy-nitrides films [13] and nitrides [14] films inactivating bacteria under visible light irradiation. Ag has been reported not to be miscible with TaN in nanocomposite films [15,16]. When using Ag-loaded textiles, silver leaching takes place and is an undesired environmental problem. Textiles with an improved Ag-adhesion are needed at the present time [17].

In this study we present: (a) the sputtering of Ag, Ta in reactive N_2/O_2 atmosphere and co-sputtering of Ta/Ag also in the presence of N_2 and O_2 on polyester, (b) the evaluation of the *Escherichia coli* inactivation kinetics on nitride and oxy-nitride films and of uniform films of Ag-nitride and Ag-oxynitride, (c) a mechanism for the photo-induced electron injection from the conduction band (cb) of Ag_2O into the conduction band (cb) of Ta_2O_5 for the TaON/Ag sample and (d) the surface characterization of the antibacterial films by up-to-date techniques.

2. Experimental

2.1. Direct current (DC) and DC-pulsed (DCP) magnetron sputtering

Direct current (DC) magnetron sputtering of metals and semiconductor oxides on diverse substrates has been recently reported by our laboratory [13,14]. Fig. 1 shows the magnetron chamber used, being the substrate-to-target distance ~10 cm. The Ta-target was two inches diameter (Lesker Hastings, East Sussex, UK). The amount of O_2 changes in the gas composition changes the appearance of the TaON films in the magnetron chamber. A reactive gas mixture 5% N_2/5% O_2/90% Ar was used in the sputtering chamber to deposit the TaON layers on the polyester and the total pressure was set at 0.1 Pa. The DC-sputtering was carried applying 280 mA and a negative bias of −330 V (90 W, current density of 12.7 mA/cm^2). The polyester samples were 2 cm × 2 cm in size.

Direct current pulsed magnetron sputtering (DCP) was used to sputter Ag on the polyester (see Fig. 1a). The Ag-target was two inches in diameter (Lesker, Hastings, East Sussex, UK). A negative voltage of −500 V was applied and then switched to +75 V (15% of −500 V). The DCP-pulses of 10 μs were applied with 280 mA, (198 W, 40 W/pulse). The calibration of films thickness for the TaON and for Ag-layers was carried out on Si-wafers with a profilometer (Alphastep500, TENCOR) and the results shown in Fig. 1b. TENCOR. The experimental values were in an error of ±10%.

The polyester was an EMPA test cloth sample No. 407. It is a polyester Dacron polyethylene–terephthalate; type 54 spun, plain weave ISO 105-F04 used for color fastness determinations. The thermal stability of Dacron polyethylene terephthalate has been reported as140 °C for times ≤1 min. The thickness of the polyester was 130 μm.

2.2. X-ray fluorescence (XRF) of the Ta/Ag-content in sputtered samples

The Ag- and Ta-content of the polyester was evaluated by X-ray fluorescence in a PANalyticalPW2400 spectrometer. Using this technique, each element emits an X-ray of a certain wavelength associated with its particular atomic number.

2.3. Diffuse reflectance spectroscopy (DRS) and irradiation procedures

Diffuse reflectance spectroscopy was carried out using a Perkin Elmer Lambda 900 UV–vis–NIR spectrometer provided for with a PELA-1000 accessory within the wavelength range of 200–800 nm
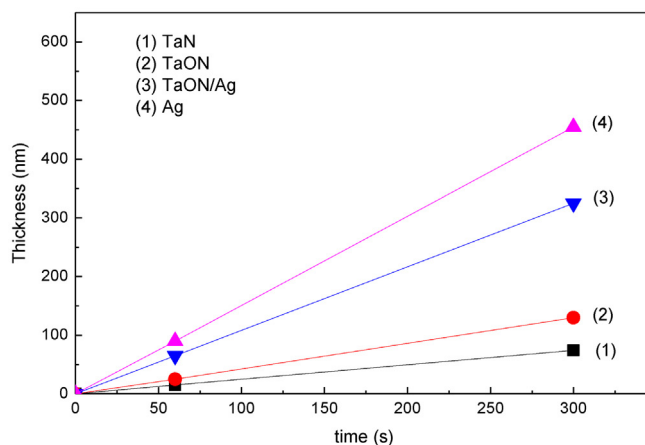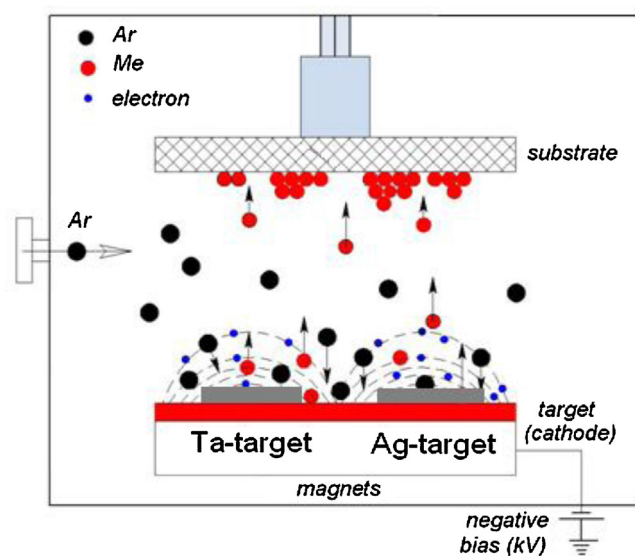

Fig. 1. (a) Schematic of the two-target direct current magnetron-sputtering chamber and (b) thickness calibration of TaN, TaON, TaON/Ag and Ag layers on Si-wafers as a function of sputtering time.

and a resolution of 1.0 nm. The absorption of the samples was plotted in Kubelka–Munk (KM) arbitrary unit *vs* wavelength.

Irradiation of the sputtered polyester samples was carried out in a tubular cavity by Osram Lumilux 18 W/827 actinic lamps. The light emitted was in the visible region (340–700 nm). Each lamp has an integral output of 1.2 mW/cm^2 and resembled the solar spectrum. These actinic lamps are used generally in hospitals and provide an efficient compromise of energy consumption per irradiated lumen. The bacterial inactivation kinetics was determined also as a function of the applied light intensity.

2.4. E. coli inactivation evaluation

The samples of *E. coli* K12 was obtained from the Deutsche Sammlung von Mikroorganismen und Zellkulturen GmbH (DSMZ) ATCC23716, Braunschweig, Germany to test the antibacterial activity of the sputtered polyester fabrics. The polyester fabrics were sterilized by autoclaving at 121 °C for 2 h. 20 μL aliquot of culture with an initial concentration of 1.4×10^6 CFU mL^{-1} in NaCl/KCl was placed on each coated and uncoated (control) polyester fabric. The samples were placed on Petri dish provided with a lid to prevent evaporation. After each determination, the fabric was transferred into a sterile 2 mL Eppendorf tube containing 1 mL autoclaved

NaCl/KCl saline solution. This solution was subsequently mixed thoroughly using a Vortex for 3 min. Serial dilutions were made in NaCl/KCl solution. A 100-μL sample of each dilution was pipetted onto a nutrient agar plate and then spread over the surface of the plate using standard plate method. Agar plates were incubated lid down, at 37 °C for 24 h before colonies were counted. The bacterial data reported were replicated three times. To verify that no re-growth of *E. coli* occurs after the total inactivation observed in the first disinfection cycle, the TaON and TaON–Ag samples were incubated for 24 h at 37 °C. Then bacterial suspension of 100 μL was deposited on 3 Petri dishes to obtain replicates of the bacterial counting. These samples are incubated at 37 °C for 24 h. No bacterial re-growth was observed. The statistical analysis of the results was performed for the decrease of the CFU values calculating the standard deviation values. The average values were compared by one-way analysis of variance and with the value of statistical significance.

2.5. Contact angle (CA) and atomic force microscopy (AFM)

The contact angles to determine the hydrophobicity of the polyester samples were assessed by means of a DataPhysics OCA 35 unit following the sessile drop.

Atomic force microscopy (AFM) of sputtered samples was performed with a Parks Scientific XE120 AFM in contact mode. The Cantilever used was an Olympus OMCL-TR400 with a spring constant 0.02 N/m. Images with a scanning field 600 nm × 300 nm were taken using a line frequency 2 Hz. The roughness was calculated using Parks' XEI software.

2.6. X-ray photoelectron spectroscopy (XPS)

An AXIS NOVA photoelectron spectrometer (Kratos Analytical, Manchester, UK) equipped with monochromatic Al Kα ($h\nu$ = 1486.6 eV) anode was used during the study. The electrostatic charge effects on the samples were compensated by means of the low-energy electron source working in combination with a magnetic immersion lens. The carbon C1s line with position at 284.6 eV was used as a reference to correct for Ag-charging effects. The quantitative surface atomic concentration of some elements was determined from peak areas using known sensitivity factors [18]. Charging effects were corrected according to Shirley [19]. Casa XPS-Vision 2 software attached to the Kratos Analytical unit deconvoluted XPS spectra.

2.7. Transmission electron microscopy (TEM)

A Philips CM-12 (field emission gun, 300 kV, 0.17 nm resolution) microscope at 120 kV was used to measure grain size of the Ag-films. The textiles were embedded in epoxy resin 45359 Fluka and the fabrics were cross-sectioned with an ultramicrotome (Ultracut E) and at a knife angle at 35°. Images were taken in Bright Field (BF) mode for the samples sputtered by DC and DCP.

3. Results and discussion

3.1. Film thickness and profilometry

Fig. 1b shows the results for the thickness calibration of sputtered TaN, TaON, Ag and co-sputtered TaON/Ag layers on the polyester. The fastest bacterial inactivation kinetics was observed for co-sputtered TaON/Ag layers for 2 min of ∼130 nm thick. This is equivalent to 650 layers. Assuming each layer with 10^{15} atoms/cm^2 a deposition rate of ∼5.4×10^{15} atoms/cm^2 s can be estimated [20]. Recent work in our laboratory showed a faster bacterial inactivation

of *E. coli* on Ag-films sputtered by DCP compared to DC-sputtered Ag-films [21].

3.2. E. coli inactivation on TaN/Ag and TaON/Ag films: effect of the light dose and bacterial concentration

The bacterial inactivation becomes faster for increasing TaN-sputtering times. Fig. 2a shows that sputtering TaN for 120 s inactivated bacteria within 300 min. Fig. 2a, trace 5) shows that in the dark no bacterial inactivation on TaN/Ag-polyester. TaN/Ag shows a faster bacterial inactivation compared to TaN films and inactivate *E. coli* within 120 min for a 120 s co-sputtered sample. Fig. 2a, traces 3 shows bacterial inactivation for TaN/Ag surfaces co-sputtered for 60 s. Since the *E. coli* inactivation time for samples sputtered for 120 s becomes shorter, a 60 s sputtering time did not deposit sufficient TaN/Ag layers or did not allow a full light absorption of the incident visible light. A sample of TaN/Ag co-sputtered for 120 shows an inactivation time of 120 min. The cosputtered TaN/Ag (150 s) sample (Fig. 2a, trace 2) is seen to inactivate *E. coli* at longer times compared to the TaN/Ag co-sputtered sample for 120 s (Fig. 2a, trace 1). This is due probably to: (a) bigger Ag-clusters hindering the diffusion of charges between TaN and the Ag layers, (b) a decrease in the number of surface catalytic sites available for bacterial inactivation [13,14], and (c) an excess of Ag acting as recombination centers for the photo-induced charges on the sample surface.

Fig. 2b shows the bacterial inactivation kinetics on TaON/Ag-polyester under O$_2$/N$_2$/Ar atmosphere. A 6 log$_{10}$ (99.99%) reduction in the bacterial concentration was observed within ∼40 min for the TaON/Ag co-sputtered sample for 120 s. Sequential sputtering of Ta and Ag lead to a slower bacterial inactivation than the co-sputtered samples as shown in Fig. 2b, trace 4. A darker gray metallic Ag-color was observed on the polyester sputtered with Ta followed by Ag. This sample was not investigated further. The Ag-sputtering on TaON leads to bigger size Ag-agglomerates hindering the efficient transfer of charges as well as light penetration into the sample [21].

The shorter bacterial inactivation kinetics reported in Fig. 2b compared to Fig. 2a can be rationalized considering that reactive sputtering in the presence of O$_2$ introduces in the TaN ionic metal–oxygen species in a matrix of covalent metal–nitrogen bonds [22]. The polarity introduced by these metal–oxygen species is due to the Van der Waals forces comprising: permanent dipoles, induced dipoles and hydrogen bonds. The surface energy of the TaON–Ag surfaces (Fig. 2b) is higher than the one available on the TaN/Ag (Fig. 2a) surface due to the presence of ionic Ag–O metal oxygen species. Fig. 2c shows that Ag sputtered on polyester does not lead to complete bacterial inactivation even after 6 h of irradiation. Fig. 2d shows that TaON samples sputtered on polyester for 120 s inactivated bacteria within 90 min. This is two times longer than the time required by TaON/Ag due to an interfacial charge transfer between Ag and TaON and this point will be discussed taking into account the optical absorption of the sample as determined by DRS spectroscopy. Fig. 2e shows the *E. coli* inactivation time as a function of the TaON/Ag layer thickness showing that a 130 nm coating leads to the shortest bacterial inactivation. For very thin TaON/Ag thicknesses below 50 nm, the microstructure of the film seems not to be effective in inducing fast bacterial inactivation kinetics. This is confirmed in Fig. 2e for coatings of 20 nm.

Fig. 3a presents the bacterial inactivation kinetics on TaON/Ag co-sputtered samples for 120 s under three different light doses from a Lumilux Osram 18 W/827 lamp. Fig. 3b shows the bacterial inactivation kinetics of *E. coli* on TaON/Ag co-sputtered samples 120 s under a Lumilux Osram 18 W/827 light for three bacterial initial concentrations. As expected the higher bacterial
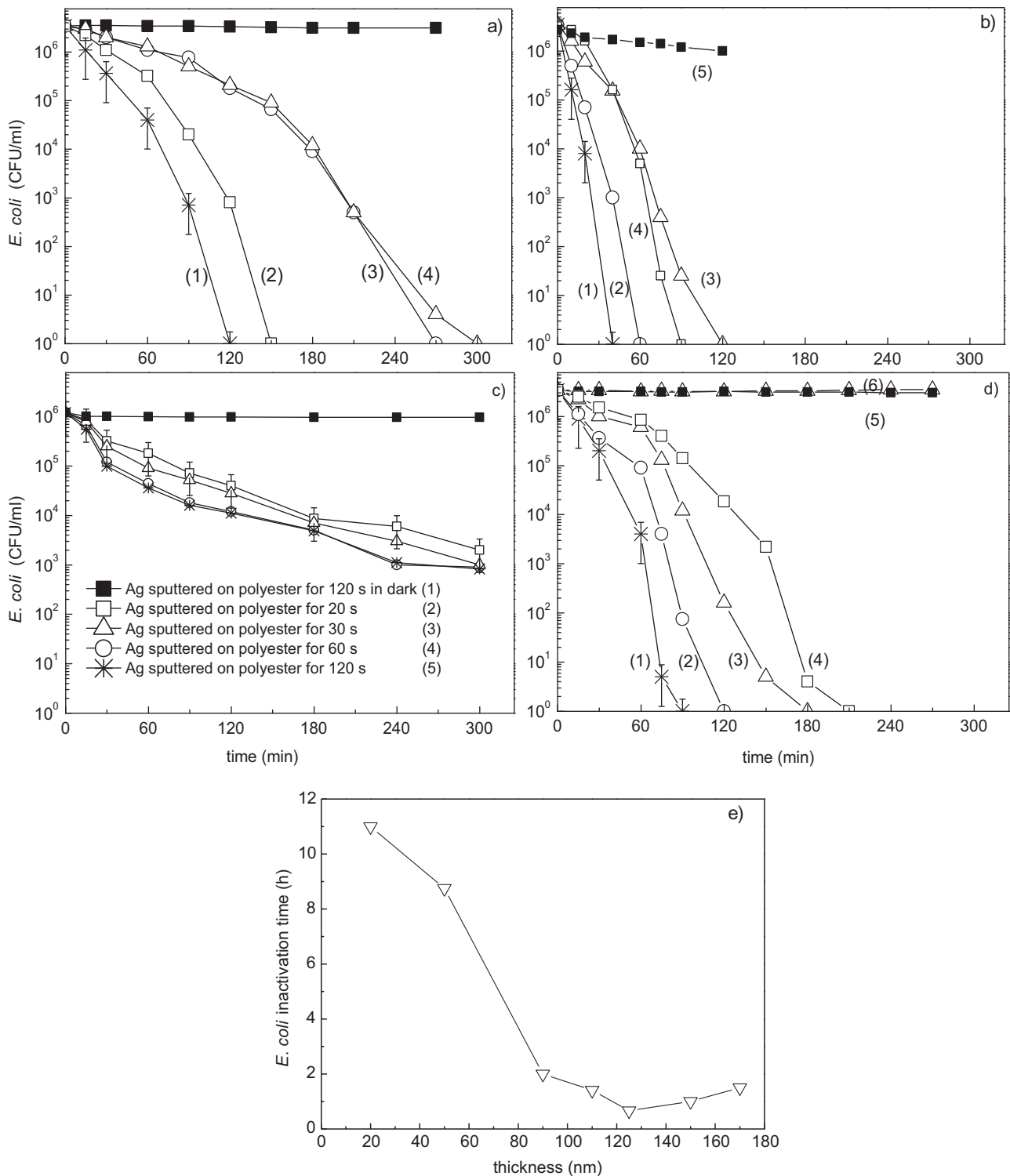
Fig. 2. *E. coli* bacterial inactivation on TaN, TaN/Ag, TaON and TaON/Ag sputtered on polyester for different times and irradiated with Osram Lumilux light (340–700 nm) with an output of 4 mW/cm². (a) (1) TaN/Ag cosputtered for 120 s; (2) for 150 s; (3) for 60 s; (4) TaN sputtered for 120 s and (5) TaN/Ag cosputtered for 120 s in dark. (b) (1) TaoN/Ag cosputtered for 120 s; (2) for 150 s; (3) for 60 s; (4) TaON/Ag sequential sputtered for 120 s TaON/40 s Ag and (5) TaON/Ag cosputtered for 120 s in dark runs. (c) See caption to traces inside the figure: Ag sputtered on polyester for different times and irradiated with Osram Lumilux light. (d) (1) TaON for 120 s; (2) TaON for 150 s; (3) TaON for 60 s; (4) TaON for 20 s; (5) TaON sputtered on polyester for 120 s in dark and (6) polyester alone irradiated with Osram Lumilux light. (e) *E. coli* bacterial inactivation as a function of the thickness of TaON/Ag film on polyester and irradiated with Osram Lumilux 18W827 actinic light.

concentration needed longer inactivation time. This observation makes it possible to exclude a strong absorption of *E. coli* on the TaON/Ag surfaces decreasing the light absorption on the film surface.

3.3. DRS of the TaON and Co-sputtered TaON/Ag samples

Fig. 4a shows the diffuse reflectance spectra of sputtered TaON. A significant shift in the absorption onset of TaON was observed
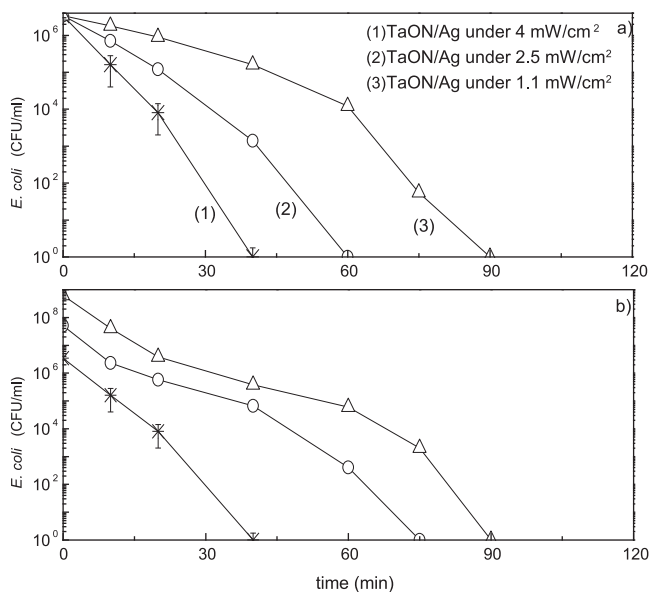
Fig. 3. *E. coli* bacterial inactivation kinetics on TaON/Ag co-sputtered on polyester: (a) effect of light dose on *E. coli* inactivation kinetics using an Osram Lumilux light (340–700 nm) and (b) effect of initial concentration of bacteria under the same light with an output of 4 mW/cm².

toward higher wavelengths. For the TaON and TON/Ag sputtered samples, the spectral intensity increases with sputtering time. For samples containing Ag in Fig. 4b, the intense spectral absorption between 400 and 600 nm is due to the localized surface resonance of the Ag-plasmons. These plasmons interacting with TaON preclude the red tail in the TaON spectra shown in Fig. 4a.

3.4. Evaluation of the Ag and Ta-contents in the TaN/Ag and TaON/Ag films

The Ag and Ta-content of the sputtered samples were determined by X-ray fluorescence (XRF) as shown in Table 1 for TaN/Ag and TaON/Ag samples. The most effective photocatalyst (TaON/Ag) co-sputtered for 120 s had a Ta-content of 0.09 wt% Ta/wt polyester and an Ag-content of 0.6 wt% Ag/wt polyester. Ag sputtered alone on polyester inactivated bacteria within longer times as shown in Fig. 2d.
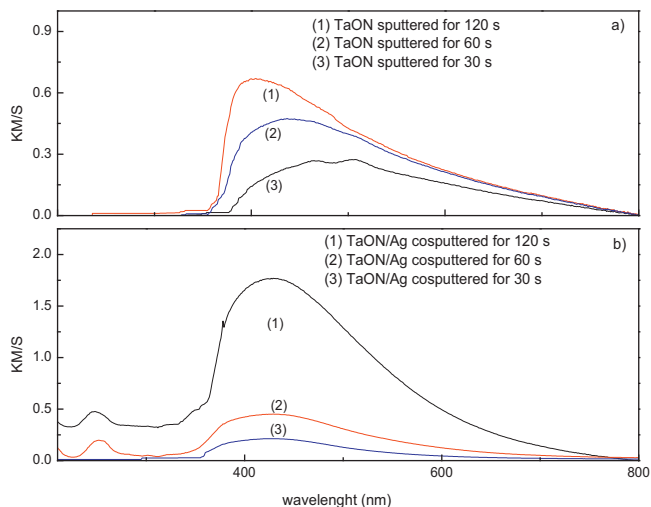

Fig. 4. Diffuse reflectance spectra in Kubelka–Munk units (a) sputtered TaON and (b) co-sputtered TaON/Ag on polyester.

Table 1
Ag- and Ta-contents as a function of sputtering times on polyester.

Samples	Sputtering time (s)	% Ag₂O wt/wt polyester	% Ta₂O₅ wt/wt polyester
TaN–Ag	40	0.0089	0.0027
	60	0.0150	0.0078
	120	0.0288	0.0131
TaON/Ag	40	0.0250	0.0147
	60	0.0471	0.0227
	120	0.0605	0.0929
	150	0.0941	0.1089

3.5. AFM and contact angle (CA) of TaON and TaON/Ag samples

Fig. 5a shows the atomic force microscopy (AFM) for a sputtered TaON (120 s) sample showing a non-uniform TaON grains with sizes of 40–60 nm. Fig. 5b shows the AFM image for a co-sputtered TaON/Ag (120 s) sample with grain sizes of 70–100 nm. The root mean square (rms) roughness for the samples TaON and TaON/Ag were respectively 2.2 and 2.7 nm. An increase in roughness leads to higher contact angle reducing the polarity and the total surface energy [23]. Increased sample rugosity allows for a better adhesion of the Ag-ions responsible for the bacterial inactivation (see Section 3.6).

The contact angles (CA) with TaON and TaON/Ag polyester as a function of time after the bacterial inactivations are shown in Fig. 6a and ba and b. The TaON sample after 2 s shows a CA of 80° and after 6 s of 12°. The water droplet disappeared after 10 s. This means that the TaON-polyester surface becomes completely hydrophilic after 10 s and eliminates any hydrophobic residues left by bacterial inactivation.
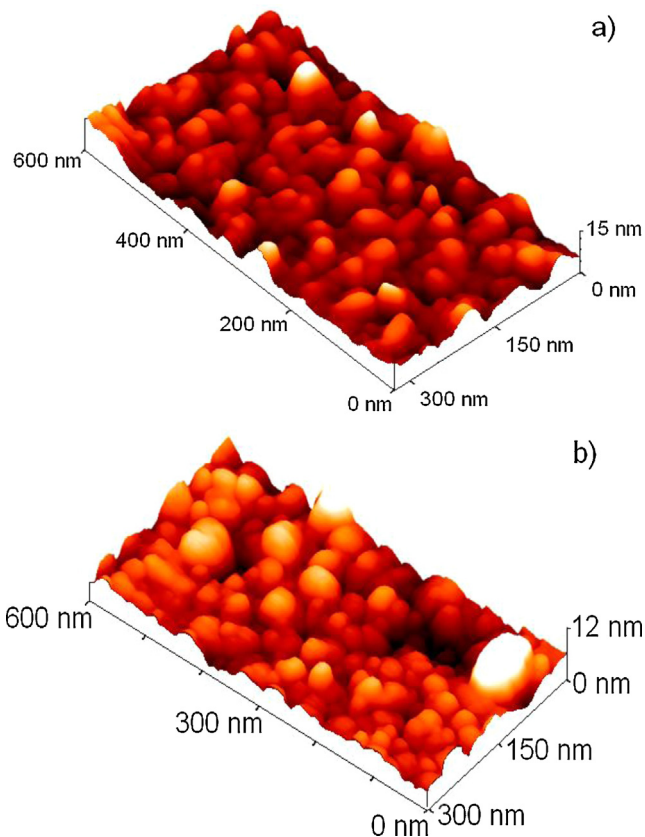

Fig. 5. Atomic force microscopy for polyester samples: (a) sputtered with TaON for 120 s time and (b) co-sputtered TaON/Ag for 120 s.
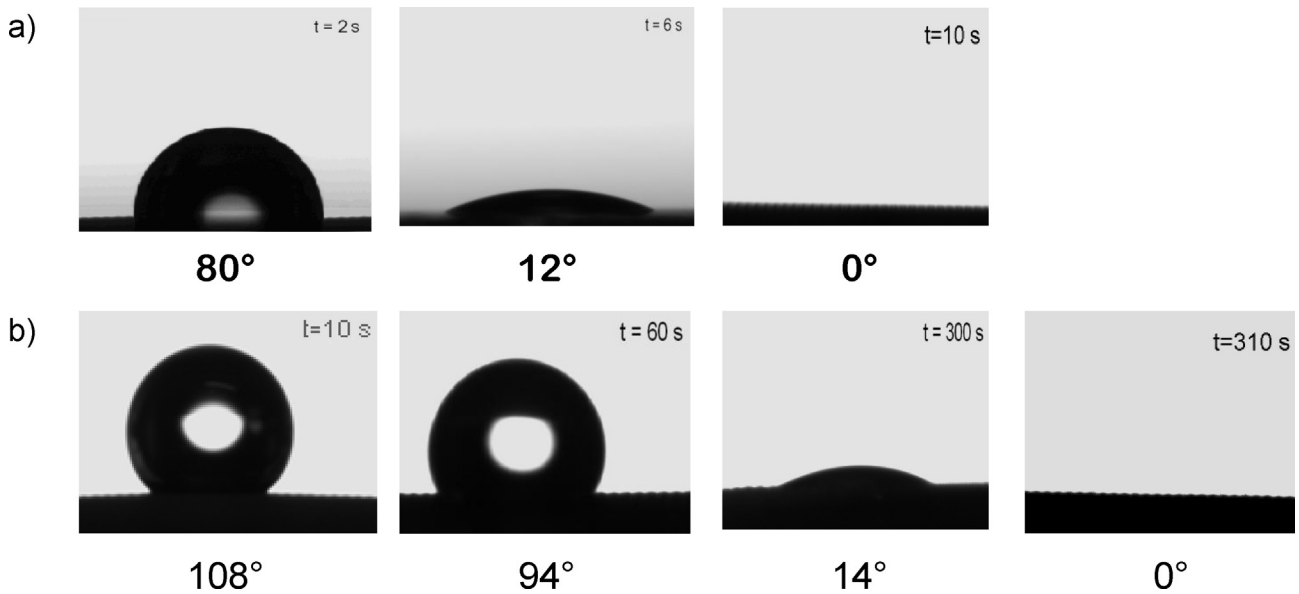
Fig. 6. Contact angle water-droplets as a function of contact time for: (a) TaON sputtered on polyester for 120 s and (b) TaON/Ag co-sputtered on polyester for 120 s.

A water droplet on the polyester alone was observed to disappear by contact with the fabric. Although the polyester is hydrophobic, the polyester has a high amount of void areas/porosity promoting water penetration through the polyester microstructure. The sputtering TaON decreases the void areas leading to water penetration and concomitly increasing the sample hydrophobicity. The amount of O_2 plays a role in the contact angle of the surface. Studies on nitrides/oxynitrides have reported that O_2 photo-adsorption introduces highly polar and electronegative groups compared to N_2 changing the electro-negativity and electron density of nitrides [12].

Fig. 6b shows the CA of the water droplet on the surface of co-sputtered TaON/Ag polyester samples. A slower decrease of the CA with time was observed on the TaON sample in Fig. 6a. The CA varied from an initial value of 108° at 10 s to 14° within 300 s and disappears completely after 310 s. The surface energy of Ta_2O_5 controls the surface CA [24]. The addition of Ag increases the hydrophobicity in the TaON/Ag film surface leading to longer absorption times for the water droplet as shown in Fig. 6b.

3.6. X-ray photoelectron spectroscopy (XPS) and spectral deconvolution

The XPS spectrum of the TaON sample is shown in Fig. 7a. The TaON spectral deconvolution of shows a peak at 24.2 eV for TaON and another peak for Ta_2O_5 at 25.9 eV, and was carried out by means of the CasaXPS-Vision 2 software. Recently, Chun et al. [23] demonstrated that TaON and Ta_2O_5 are stable species able to carry oxidation/reduction reactions under visible light.

Fig. 7b shows the Ag 3d5/2 doublet with a split of 6 eV found in the co-sputtered TaON/Ag films for 40 s, 60 s and 120 s. Values for the Ag Auger parameter in Table 2 present the oxidation state of

silver. The shift in BE from 364.4 eV to 364.9 eV was due to the shift of the peaks of AgO to Ag_2O and Ag^0 as a function of sputtering times of 40 s, 60 s and 120 s respectively [18]. For the initial sputtering of 40 s, the Auger parameter was found at 725.15 eV and the Ag^0
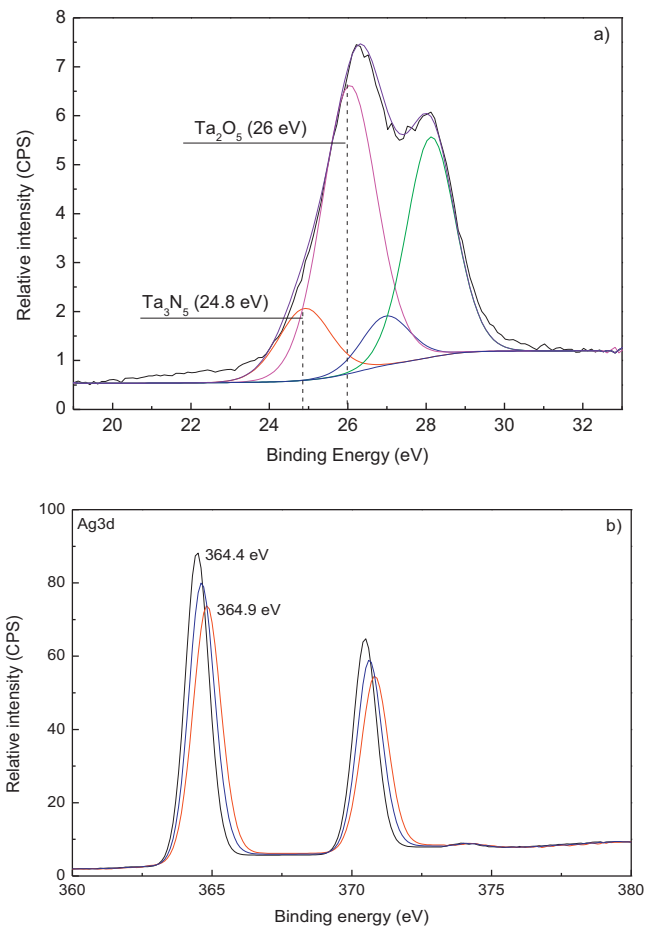

Fig. 7. (a) XPS spectra of Ta4f in TaON sputtered films and (b) Ag deconvolution in the co-sputtered TaON/Ag at 40 s, 60 s and 120 s films.

Table 2
Surface atomic concentration percentage of elements during *E. coli* inactivation on TaON–Ag polyester (120 s) co-sputtered sample under light.

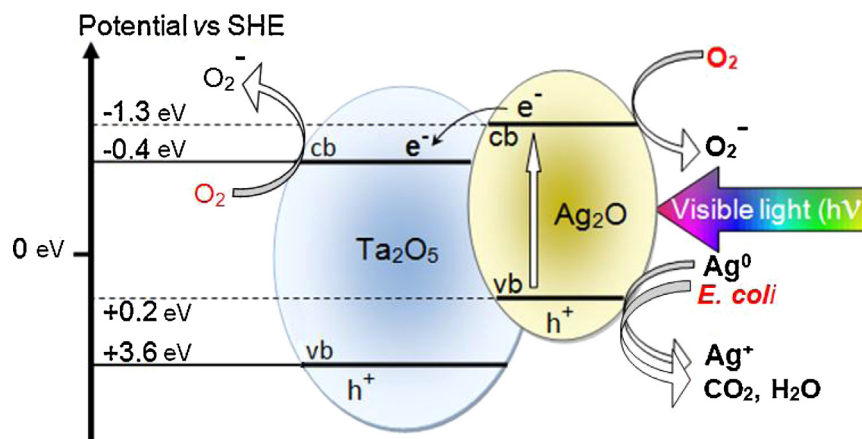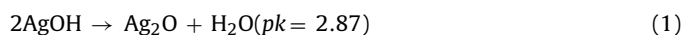|	O1s	Ta4f	N1s	Ag3d	C1s
$t = 0$	22.13	12.04	4.47	21.50	23.71
$t = 0$ contacted bacteria	31.24	9.67	2.74	14.08	42.28
$t = 20$ min	24.09	10.51	3.02	20.11	34.22
$t = 40$ min	19.55	12.21	4.48	20.79	28.76

Fig. 8. Scheme for the photoinduced interfacial charge transfer (IFCT) from Ag_2O to Ta_2O_5 under visible light irradiation.

content of the TaON sample is very low. At longer deposition times, the Auger parameter at 725.65 eV suggests the formation of Ag^0 along a low amount of ionic silver. To separate the ionic states of Ag is not a simple matter due to the electrostatic charging of the sample but shifts of 0.2 eV or more are generally accepted as evidence for the change in the electronic configuration of a species detected by XPS [24]. Values for the Ag Auger parameter in Table 3 present the oxidation state of silver.

The TaON/Ag surface binds the protein N-amides I/II, carboxylic and S-groups of the bacterial cell wall containing negative surface charged functional groups [3,4]. The Ag-ions react with the bacterial cell-wall leadings to cell damage and bacterial inactivation as reported in Fig. 2a–e.

3.7. Suggested mechanism for the photo-induced IFCT process

The photo-induced interfacial charge transfer from the Ag-layers to the TaON layers will be discussed in this section. Visible light is absorbed by the narrow band semiconductor Ag_2O up to 880 nm and the wide band semiconductor Ta_2O_5 absorbs UV-light < 310 nm. In Fig. 8, a mechanism for electron injection for the charge transfer from Ag_2O into Ta_2O_5 is suggested. This mechanism considers the potential energy of the semiconductor bands [23]. When the sputtered Ag layer is exposed to air, the water vapor in the air leads to the formation of surface AgOH. The AgOH has been reported to decompose spontaneously to Ag_2O (Eq. (1)) [24].

$$2AgOH \rightarrow Ag_2O + H_2O (pk = 2.87) \tag{1}$$

Ag_2O is thermodynamically stable at pH 6–7. This is the pH range at which the bacterial inactivation proceeds in Fig. 2a–d. The Ag_2O has been reported with a cb at −1.3 eV NHE (pH 0), vb at +0.2 V NHE (pH 0) and bg of 1.5 eV. The wide band-gap semiconductor Ta_2O_5 has been reported with a cb at −0.4 V, vb at +3.6 V NHE (pH 0) and a bg of 4.0 eV [23].

The electron injection from Ag_2O to the Ta_2O_5 is thermodynamically favorable. The Ag_2O (cb) at −1.3 eV NHE lays above the Ta_2O_5 cb at 0.4 eV NHE. The potential 1.7 eV difference in provides a considerable driving force inducing a fast electron injection from Ag_2O into Ta_2O_5. Due to the magnitude of this driving potential the Ag_2O transfers the majority of the electrons to the Ta_2O_5 cb hindering the e^-/h^+ recombination in Ag_2O. The values for the potentials for the cb for both semiconductors are only indicative, since in quantum size nanoparticles, the band energy shifts have been reported to higher potentials [25,26]. The reductive character in the quantum size Ag_2O particles proceeds at a higher energy level than −1.3 eV NHE. The potential energy of the h^+ at the vb of Ta_2O_5 (3.6 eV) becomes more positive than the standard

reduction potential of $HO^\bullet/HO^-$ of ~1.9 eV [3]. The vb holes h^+ will oxidize the Ta_2O_5 surface-OH to $OH^\bullet$ and this radical subsequently oxidizes E. coli (see Fig. 8) [3,4]. The IFCT charge transfer would be favored by the close contact between Ag and Ta-particles sample in the co-sputtered TaON/Ag (120 s) sample (see in Fig. 9). The higher activity of the coupled semiconductors may be also due to a higher density of defects in their crystallites.

Under visible light irradiation Ag_2O gives raise to the charge separation

$$Ag_2O + visiblelight \rightarrow h^+ + e^- \tag{2}$$

$$Ag_2O + e^- \rightarrow 2Ag^0 + O^- \tag{3a}$$

$$Ag_2O + e^- \rightarrow 2Ag^0 + 1/2O_2 \tag{3b}$$

The electron injection from the Ag_2O cb to the Ta_2O_5 (cb) hinders the charge recombination in Ag_2O upon visible light excitation in Eq. (2). Concomitantly, the cb e^- become available to reduce oxygen in Eq. (3a). The photo-induced electron Eq. (3b) lead to silver atoms and additionally produce highly oxidative radicals Eqs. (5) and (6). The (vb)h^+ Eq. (2) reacts with H_2O in Eq. (4) leading to $OH^\bullet$ radicals or other highly oxidative oxidative radicals in Eq. (5)

$$h^+ + H_2O \rightarrow OH^\bullet + H^+ \tag{4}$$

$$e^- + H_2O + 1/2O_2 \rightarrow OH^\bullet + OH^- \tag{5}$$

$$e^- + O_2 \rightarrow O_2^- \tag{6}$$

Within the band-gap of each semiconductor there are intermediate electron transitions between the cb and the vb band. More information is needed about these indirect transitions at the present time. Studies have reported visible light induced electron injection from Ag into TiO_2 leading to surface Ag^0/Ag_2O.

3.8. Electron microscopy of polyester modified samples (TEM)

Fig. 9 presents the TEM of (a) the polyester sample and (b) the TEM of a TaON/Ag co-sputtered sample showing the Ta_2O_5 clearer particles presenting sizes 5–8 nm. The Ag-particles were found to be 10–16 nm (counting for 100 particles) with an interfacial particle distance up to 10 nm between Ta_2O_5 and Ag_2O. The close contact in the co-sputtered TaON/Ag sample compared to the samples sputtering sequentially TaON and Ag, a closer contact between both occurs inducing higher quantum efficiency. This led to shorter bacterial inactivation times for the co-sputtered samples compared to the sequentially sputtered sample.
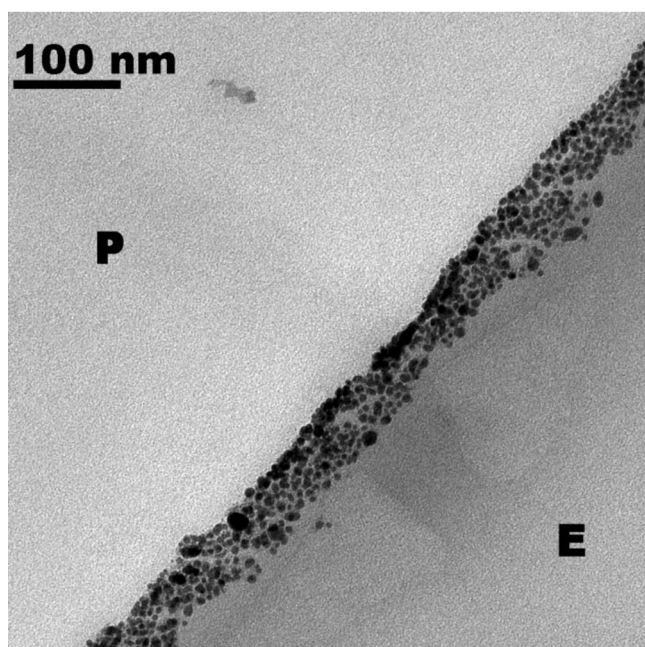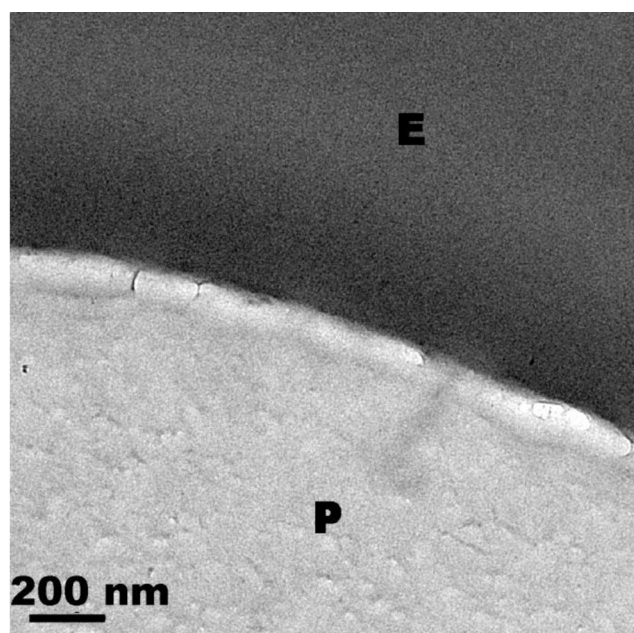
Fig. 10. Recycling of TaON/Ag (120 s) during *E. coli* bacterial inactivation for 5 cycles: (1) first cycle; (2) third cycle and (3) fifth cycle.

Table 3
Auger parameters of Ag in co-sputtered TaON/Ag samples.

Sputtering time (s)	Auger parameters of Ag (eV) [13,21]	Auger parameters of Ag in the co-sputtered TaON/Ag samples (eV)
40	725.15	725.15
60	725.15	725.53
120	725.52	725.65
150	725.65	725.66

presenting a microstructure able to: (a) preclude to some extent electron–hole recombination [22], (b) further the interfacial transfer (IFCT) between Ag_2O and Ta_2O_5 and (c) improve the charge transfer between the film and the bacterial surface [12,13,22,26].

3.9. Recycling of the sputtered polyester samples

The recycling of the co-sputtered TaON/Ag (120 s) sample up to the 5th cycle is seen in Fig. 10. It proceeds with no significant loss in activity since the bacterial inactivation time remained the same. The sample was thoroughly washed after each recycling experiment. The reuse of the co-sputtered TaON/Ag samples is possible since total bacterial destruction was attained at each cycle. The total destruction of the bacterial residues enables a stable sample recycling due to the TaON/Ag-samples self-clean as shown in Table 2. The N- and C-bacterial residues did not accumulate on the polyester due to the rapid catalytic destruction of these elements on the photocatalyst surface. A slow increase in the C-content with time is shown in Table 2 within the time of bacterial inactivation. This is due to adventitious hydrocarbons spontaneously adsorbed from the air on the film surface, while O, Ta, N, Ag percentage surface concentration remains stable. A further proof of the surface self-cleaning is provided by the contact angle shown in Fig. 6b. The fact that the CA vanishes after 310 s indicates that no hydrophobic compounds remain on the sample surface after the bacterial inactivation (Table 2).

4. Conclusions

TaON and TaON/Ag films on polyester are shown to be able to inactivate bacteria in the minute range under low intensity visible/actinic light (340–700 nm) light. The fastest inactivation kinetics within 40 min was obtained with TaON/Ag-polyester co-sputtered samples for 120 s. By XPS spectral deconvolution Ta_2O_5 and Ag_2O were identified in the TaON/Ag photocatalyst. Evidence is presented for the interfacial charge transfer mechanism (IFCT) between Ag_2O and Ta_2O_5. The Ag-species is the visible light

Fig. 9. Electronic microscopy of: (a) polyester fiber and (b) sputtered TaON/Ag (120 s) film on polyester (E: epoxy, P: polyester).

Small particles of less than 10 nm as shown in Fig. 9 show different properties from those in bulk materials. The quantum size effect is applicable to particles with sizes 10 nm having about 10^4 atoms [3]. The quantum size nature of the semiconductors particles has been reported to introduce a marked perturbation in their band structure [3,12,26].

Donor–acceptor interactions depend on the charge diffusion distance and this distance is a function of the particle size and shape. But unfavorable effects associated with small size are also known and cannot be discounted in our samples. First, the recombination time for the induced charges on Ag_2O becomes shorter due to the decrease of the available space for the charge separation and second, the decrease of the space charge layer with the consequent decrease in potential depth. Nevertheless, the co-sputtered samples lead to fast inactivation kinetics (Fig. 2b)
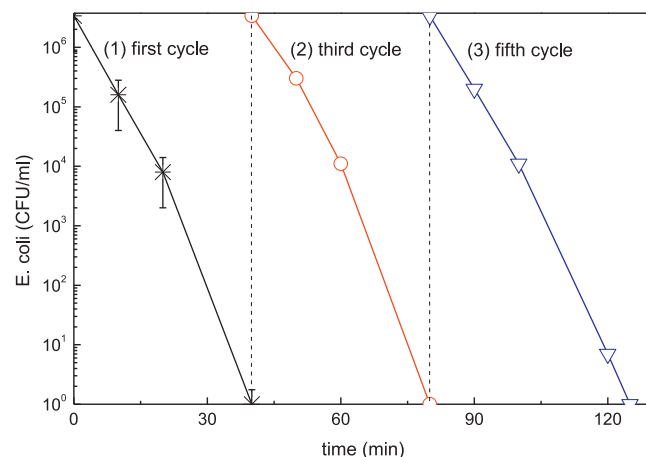
absorber and transfers the photo-induced charges to Ta_2O_5. AFM and TEM of the sputtered films show a uniform coating of TaON/Ag layers on polyester. Contact angle (CA) and X-ray fluorescence were also carried out to characterize the surface of the TaON and TaON/Ag layers.

Acknowledgments

References

[1] Thüringer Surface and Biomaterials Kolloquium, 13/15 September 2012, Zeulenroda, Germany.
[2] A. Kramer, I. Schwebke, G. Kampf, How long do socomial pathogens persist in on inanimate surfaces? BMC Infect. Dis. 130 (2006) 137–146.
[3] A. Mills, C. Hill, P. Robertson, Overview of the current ISO tests for photocatalytic materials, J. Photochem. Photobiol. A 237 (2012) 7–23.
[4] K. Page, M. Wilson, P.I. Parkin, Antimicrobial surfaces and their potential in reducing the role of the inanimate environment in the incidence of hospital-acquired infections, J. Mater. Chem. 19 (2009) 3819–3831.
[5] S. Noimark, Ch. Dunnill, M. Wilson, P.I. Parkin, The role of surfaces in catheter-associated infections, Chem. Soc. Rev. 38 (2009) 3435–3448.
[6] P.I. Parkin, G.R. Palgrave, Self-cleaning coatings, J. Mater. Chem. 15 (2005) 1689–1695.
[7] K. Page, R. Palgrave, P.I. Parkin, M. Wilson, Sh. Savin, A. Chadwick, Titania and siver titania composite films on glass-potent antimicrobial coatings, J. Mater. Chem. 17 (2007) 95–104.
[8] H.A. Foster, P. Sheel, W.D. Sheel, P. Evans, S. Varghese, N. Rutschke, M.H. Yates, Antimicrobial activity of titania/silver and titania/copper films prepared by CVD, J. Photochem. Photobiol. A 216 (2010) 283–289.
[9] M.S.P. Dunlop, P.C. Sheeran, A.J. Byrne, S.A. McMahon, M.A. Boyle, G.K. McGuigan, Inactivation of clinically relevant pathogens by photocatalytic coatings, J. Photochem. Photobiol. A 216 (2010) 303–3010.
[10] M.H. Yates, A.L. Brook, B.I. Ditta, P. Evans, H.A. Foster, D.W. Sheel, A. Steele, Photo-induced self-cleaning and biocidal behviour of titania and copper oxide multilayers, J. Photochem. Photobiol. A 197 (2008) 197–208.
[11] R. Asahi, T. Morikawa, T. Ohwaki, K. Aoki, Y. Taga, Visible-light photocatalysis in nitrogen-doped titanium oxides, Science 293 (2001) 269–273.
[12] M. Mohamed, D. Bahneman, The role of electron transfer in photocatalysis: fact and fictions, Appl. Catal. B 128 (2012) 91–104.
[13] S. Rtimi, O. Baghriche, R. Sanjines, C. Pulgarin, M. Ben-Simon, J-C. Lavanchy, A. Houas, J. Kiwi, Photocatalysis/catalysis by innovative TiN and TiN–Ag surfaces inactivate bacteria under visible light, Appl. Catal. B 123–124 (2012) 306–313.
[14] S. Rtimi, O. Baghriche, O. Pulgarin, R. Sanjines, J. Kiwi, Design, testing and characterization of innovative TiN–TiO₂ surfaces inactivating bacteria under low intensity visible light, RSC Adv. 2 (2012) 8591–8595.
[15] P. Kelly, H. Li, P. Benson, K. Whitehead, J. Verran, R. Arnell, I. Iordanova, Comparison of the tribological and antimicrobial properties of CrN/Ag, ZrN/Ag, TiN/Ag and TiN/Cu nanocomposite coatings, Surf. Coat. Technol. 205 (2010) 1606–1610.
[16] P. Kelly, H. Li, K. Whitehead, J. Verran, R. Arnell, I. Iodornova, A study of the antimicrobial and tribological properties of TiN/Ag nanocomposite coatings, Surf. Coat. Technol. 204 (2009) 1137–1141.
[17] L. Geranio, M. Heuberger, E. Nowack, The behavior of silver nano textiles during washing, Environ. Sci. Technol. 43 (2009) 8113–8118.
[18] D. Wagner, M. Riggs, E. Davis, G. Müllenberg (Eds.), Handbook of X-ray Photoelectron Spectroscopy, Perkin-Elmer Corporation, Physical Electronics Division, Minnesota, 1979.
[19] D.A. Shirley, High-resolution X-ray photoemission spectrum of the valence bands of gold, Phys. Rev. B 5 (1972) 4709–4716.
[20] J. Mathews, Epitaxial Growth Part B, IBM Thomas Watson Research Center, Academic Press, New York, 1975, pp. 382–436.
[21] O. Baghriche, R. Sanjines, C. Ruales, C. Pulgarin, I. Stolitchnov, A. Zertal, J. Kiwi, Ag-surfaces sputtered by DC and pulsed DC-magnetron sputtering effective in bacterial inactivation: testing and characterization, Surf. Coat. Technol. 206 (2011) 2410–2416.
[22] C. Creutz, S. Bruce, S. Brunschwig, S. Sutin, Interfacial charge transfer absorption: application to metal–molecule assemblies, Chem. Phys. 324 (2006) 244–258.
[23] W. Chun, A. Ishikawa, H. Fujisawa, T. Takata, N. Kondo, M. Hara, M. Kawai, Y. Matsumoto, K. Domen, Conduction and valence band positions of Ta₂O₅, TaON, and Ta₃N₅ by UPS and electrochemical methods, J. Phys. Chem. B 107 (2003) 1798–1803.
[24] G. Biedermann, G. Sillen, Studies on the hydrolysis of metal ions. Part 30. A critical survey of the solubility equilibria of Ag₂O, Acta Chem. Scand. 14 (1960) 07–17.
[25] Y. Ida, T. Watase, M. Shinagawa, M. Watabanbe, M. Chigane, M. Inaba, A. Tasaka, M. Izaki, Direct electrodeposition of 1.46 eV bandgap silver(I) oxide semiconductor films by electrogenerated acid, Chem. Mater. 20 (2008) 1254–1256.
[26] A. Nozik, Photoeffects at the semiconductor electrolyte interface, in: ACS Symp. Ser. 140, Amer. Chem. Soc., Washington, 1990.